

## Letter

# A simple model for doublet bands in doubly odd nuclei

N. Yoshinaga<sup>1,a</sup> and K. Higashiyama<sup>2,3</sup>

<sup>1</sup> Department of Physics, Saitama University, Saitama City 338-8570, Japan

<sup>2</sup> Department of Physics, Chiba Institute of Technology, Narashino, Chiba 275-0023, Japan

<sup>3</sup> Department of Physics, University of Tokyo, Hongo, Tokyo 113-0033, Japan

Received: 10 August 2006 / Revised: 28 September 2006 /

Published online: 15 November 2006 – © Società Italiana di Fisica / Springer-Verlag 2006

Communicated by S. Kubono

**Abstract.** Nuclear structure of doublet bands in doubly odd nuclei with mass  $A \sim 130$  is investigated within the framework of a simple model where the even-even core couples with a neutron and a proton in intruder orbitals through a quadrupole-quadrupole interaction. The model reproduces quite well the energy levels of doublet bands and electromagnetic transitions. The staggering of the ratios  $B(M1; I \rightarrow I-1)/B(E2; I \rightarrow I-2)$  of the yrast bands turns out to be described by the chopsticks-like motion of two angular momenta of the unpaired neutron and the unpaired proton when they are weakly coupled with the core.

**PACS.** 21.60.-n Nuclear structure models and methods – 23.20.Lv  $\gamma$  transitions and level energies – 27.60.+j  $90 \leq A \leq 149$

One of the most intriguing phenomena discussed in medium and heavy nuclei is the appearance of the nearly degenerate doublet bands in doubly odd nuclei. Such pairs of bands built on the  $\nu h_{11/2} \otimes \pi h_{11/2}$  configuration have been experimentally found in many doubly odd nuclei in the mass  $A \sim 130$  region [1–6]. Previously these bands were interpreted as a manifestation of the chiral doublet bands [7]. However, many of recent experiments and analyses do not support this interpretation [8–12]. Recently, we have proposed a pair truncated shell model (PTSM) where the even-even core made of the collective pairs couples with a neutron and a proton in high- $j$  intruder orbitals [13–15]. The PTSM successfully describes the properties of doubly odd nuclei in the mass  $A \sim 130$  region, *i.e.*, both energy spectra and features of electromagnetic transitions. Now the band structure of the doublet bands is well explained by the chopsticks-like motion of two angular momenta of the odd neutron and the odd proton, weakly coupled with the core. Since the PTSM results are rather complicated to analyze, we need a further simplified model to pinpoint the essential mechanism more closely.

In this letter we propose a quadrupole coupling model (QCM) where the even-even collective core couples with a neutron and a proton in the high- $j$  intruder orbitals through a quadrupole-quadrupole interaction, and we apply this model to the doublet bands in the mass  $A \sim 130$  region. In the region, several valence proton particles and

valence neutron holes are coupled to the doubly magic nucleus  $^{132}\text{Sn}$ . In the QCM, the states of doubly odd nuclei (neutron number  $N$  and proton number  $Z$ ) with the  $\nu h_{11/2} \otimes \pi h_{11/2}$  configuration are assumed to be constructed by a neutron hole, a proton particle in the  $0h_{11/2}$  intruder orbitals, and a collective core. The core is assumed to be made of  $N+1$  neutrons and  $Z-1$  protons. A system of one neutron hole in the orbital  $j_\nu$  and one proton particle in the orbital  $j_\pi$  is specified as the state  $|j_\nu j_\pi; L\rangle$ , where  $L$  is the angular momentum of the particle-hole state. The collective-core state is denoted as  $|R\rangle$ , where  $R$  indicates the angular momentum of the core state. In the simplest version of the model we assume that the neutron and the proton outside the core couple only with the yrast states of the core. Then, a total wave function of any doubly odd nucleus is written as a product of the collective-core state and the particle-hole state,

$$|\Phi(RL; I)\rangle = [|R\rangle \otimes |j_\nu j_\pi; L\rangle]^{(I)}, \quad (1)$$

where  $I$  is the total spin. We assume that the model Hamiltonian can be written as

$$H = H_{core} + H_{c\nu} + H_{c\pi} + H_{\nu\pi}, \quad (2)$$

where  $H_{core}$  indicates the Hamiltonian of the collective core,  $H_{c\nu}$ , the interaction between the collective core and the neutron hole,  $H_{c\pi}$ , between the collective core and the proton particle, and  $H_{\nu\pi}$ , between the neutron hole and the proton particle.

<sup>a</sup> e-mail: yoshinaga@phy.saitama-u.ac.jp

We determine the Hamiltonian of the collective core via matrix elements as

$$\langle R | H_{core} | R' \rangle = E_R \delta_{RR'}, \quad (3)$$

where  $E_R$  is provided by the experimental excitation energy of the yrast state with spin  $R$  in the even-even nucleus with  $N + 1$  neutrons and  $Z - 1$  protons. We also assume that the other interactions,  $H_{c\nu}$ ,  $H_{c\pi}$ , and  $H_{\nu\pi}$ , are of pure quadrupole-quadrupole types

$$H_{c\nu} = \kappa_{c\nu} Q_c \cdot Q_\nu, \quad (4)$$

$$H_{c\pi} = \kappa_{c\pi} Q_c \cdot Q_\pi, \quad (5)$$

$$H_{\nu\pi} = \kappa_{\nu\pi} Q_\nu \cdot Q_\pi, \quad (6)$$

where  $\kappa$ 's are the interaction strengths, and  $Q_c$ ,  $Q_\nu$ , and  $Q_\pi$  indicates the quadrupole operator for the core, a neutron hole and a proton particle, respectively. Here, the quadrupole operator for the collective core,  $Q_c$ , is defined through the reduced matrix element as

$$\langle R' || Q_c || R \rangle = \sqrt{(2R' + 1)(2R + 1)} (R0R'0 | 20), \quad (7)$$

where  $(R0R'0 | 20)$  stands for a Clebsch-Gordan coefficient. The quadrupole operator for the neutron and proton in a single- $j$  shell,  $Q_\tau$  ( $\tau = \nu$  or  $\pi$ ), is defined in terms of the reduced matrix element as  $\langle j || Q || j \rangle = 1$ , since it is not relevant for determining energy spectra.

Electromagnetic transition operators consist of three parts, *i.e.*, the collective core, the neutron, and the proton parts. Then the  $E2$  transition operator is defined as

$$T(E2) = e_c Q_c + e_\nu Q_\nu + e_\pi Q_\pi, \quad (8)$$

where  $e_c$ ,  $e_\nu$ , and  $e_\pi$  represents the effective charge of the collective core, neutrons, and protons, respectively. The  $M1$  transition operator is defined as

$$T(M1) = g_c R + g_{\ell\nu} \ell_\nu + g_{s\nu} s_\nu + g_{\ell\pi} \ell_\pi + g_{s\pi} s_\pi, \quad (9)$$

where  $g_c$  stands for the  $g$ -factor of the collective core,  $g_{\ell\nu}$  ( $g_{s\nu}$ ) and  $g_{\ell\pi}$  ( $g_{s\pi}$ ) represent the  $g$ -factors for orbital angular momentum (spin) for neutrons and protons, respectively. The operators  $R$ ,  $\ell$ , and  $s$  represent the angular momentum of the core, the orbital angular momentum of the neutron hole and proton particle, and the spin of the neutron hole and proton particle, respectively. For further details the model is explained in a forthcoming paper.

In order to calculate the energies of the yrast and yrare states with the  $\nu h_{11/2} \otimes \pi h_{11/2}$  configuration, the Hamiltonian of eq. (2) is diagonalized in terms of the basis states of eq. (1) as

$$H |\Phi(I\eta)\rangle = E_{I\eta} |\Phi(I\eta)\rangle, \quad (10)$$

where  $|\Phi(I\eta)\rangle$  and  $E_{I\eta}$  are normalized eigen-vectors and eigen-energies, respectively, and  $\eta$  is an additional quantum number required to completely specify the state. As for the excitation energies of the collective core,  $E_R$ , we adopt the experimental energies of the yrast  $0^+$ ,  $2^+$ ,  $4^+$ ,  $6^+$ ,  $8^+$  and  $10^+$  states for the even-even nuclei ( $N + 1$ ,  $Z - 1$ ). Since the energies of the yrast  $6^+$ ,  $8^+$  and  $10^+$  states for  $^{132}\text{Xe}$  are not experimentally confirmed, we use mean energies of the corresponding levels in  $^{130}\text{Xe}$  and  $^{134}\text{Xe}$ .

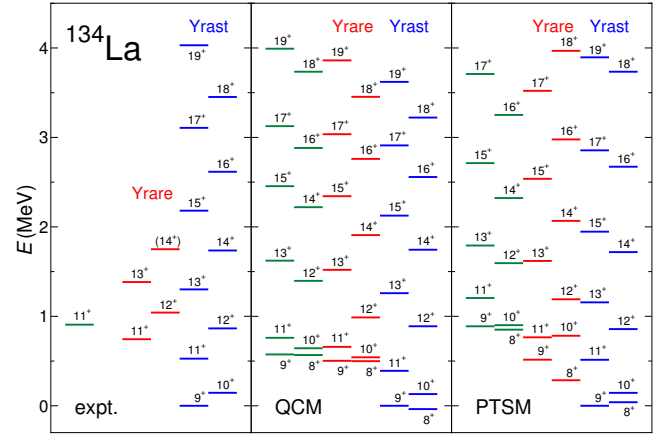


**Fig. 1.** Comparison of experimental energy levels (expt.) with the QCM results (QCM), and those in the PTSM (PTSM) for  $^{134}\text{La}$ . Experimental data are taken from ref. [2], and the PTSM results from ref. [14].

The interaction strengths,  $\kappa_{c\nu}$ ,  $\kappa_{c\pi}$ , and  $\kappa_{\nu\pi}$ , are determined to reproduce both the experimental energy spectra and the ratios  $B(M1; I \rightarrow I - 1)/B(E2; I \rightarrow I - 2)$  for the doubly odd nuclei in the mass  $A \sim 130$  region. The strengths are assumed to be smoothly changed as functions of the neutron number  $N$  and the proton number  $Z$ . The determined functional dependences are given as follows (in unit of MeV):

$$\begin{aligned} \kappa_{c\nu} &= -0.30(Z - 50) + 0.25(N - 82) + 2.55, \\ \kappa_{c\pi} &= 0.10(Z - 50) - 0.05(N - 82) - 1.35, \\ \kappa_{\nu\pi} &= 0.50(Z - 50) + 2.50. \end{aligned} \quad (11)$$

In fig. 1, the energy spectrum obtained by the QCM is compared with experiment for  $^{134}\text{La}$ . The model reproduces well the energy levels with spins less than 16. In experiment the  $8_1^+$  state is not observed, but the QCM calculation predicts the  $8_1^+$  state to lie near the  $9_1^+$  state. Concerning the high-spin states ( $I \geq 16$ ), their level spacings are smaller compared to the experimental data. Note that the even-even nucleus  $^{134}\text{Ba}$  (the collective core of  $^{134}\text{La}$ ) has an irregular yrast sequence due to band crossing, so that in addition to the yrast states, yrare states of the core might be necessary to describe such high-spin states. In fig. 1, the energy levels of the PTSM taken from ref. [14] are also shown in comparison with those of the QCM and experiment. The calculated energy levels with spins less than 16 are in good agreement with experiment. In contrast to the QCM results, the theoretical  $8_1^+$  state is in between  $9_1^+$  and  $10_1^+$  states. The theoretical level spacings between the  $16_1^+$  and  $18_1^+$  states, and between the  $17_1^+$  and  $19_1^+$  states are larger compared to the QCM results.

In fig. 2 and fig. 3, the theoretical energy levels of the QCM are compared with the experimental data for  $^{128}\text{Cs}$ ,  $^{130}\text{La}$ ,  $^{136}\text{Pr}$  and  $^{134}\text{Pr}$ . For  $^{128}\text{Cs}$ , the theoretical level spacing between the  $9_1^+$  and  $11_1^+$  states is smaller compared to experiment. However, our calculation reproduces the relative positions of the yrast and yrare states with spins greater than 11. For  $^{130}\text{La}$ , we obtain an excellent

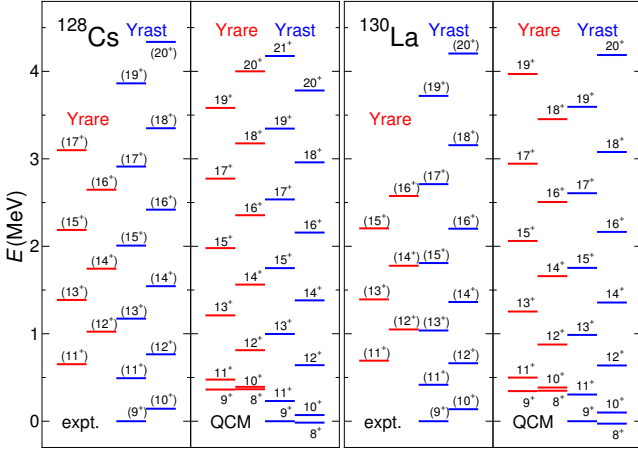


**Fig. 2.** Comparison of the experimental energy levels (expt.) with those of the QCM (QCM) for  $^{128}\text{Cs}$  and  $^{130}\text{La}$ . Experimental data are taken from refs. [4, 16].

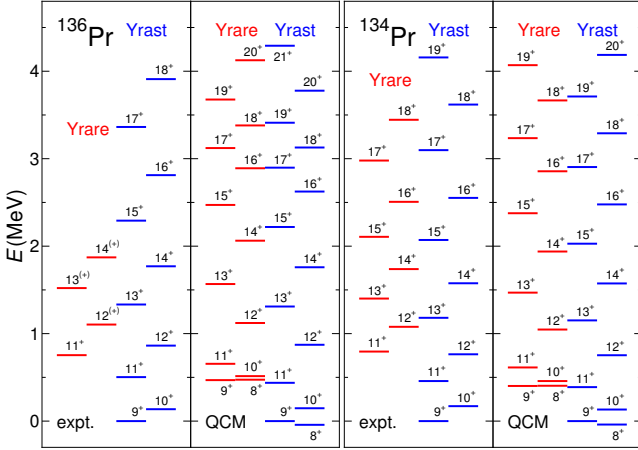


**Fig. 3.** The same for  $^{136}\text{Pr}$  and  $^{134}\text{Pr}$  as in fig. 2. Experimental data are taken from refs. [17, 18].

agreement with the experimental data. As for Pr isotopes, the spin assignment in the figure is changed from that claimed in experiment by one (from  $I$  to  $I + 1$ ) because the experimental assignment is thought to be unnatural from our theoretical point of view. For  $^{136}\text{Pr}$  and  $^{134}\text{Pr}$ , the QCM reproduces well the energy levels with spins less than 16. In  $^{136}\text{Pr}$ , the level spacings for high-spin states are smaller compared to experiment, which arises due to the irregular level sequence in the yrast band of  $^{136}\text{Ce}$ . For  $^{134}\text{Pr}$ , excellent agreements with the experimental data are achieved for the energy levels of the high-spin states.

The effective charge of the collective core in eq. (8) is determined by the  $B(E2; 2_1^+ \rightarrow 0_1^+)$  value of the even-even nucleus ( $N + 1, Z - 1$ ) as

$$|e_c| = \sqrt{B(E2; 2_1^+ \rightarrow 0_1^+)}. \quad (12)$$

The adopted  $B(E2; 2_1^+ \rightarrow 0_1^+)$  values are 0.092, 0.130, 0.150, 0.134, 0.172, 0.233, 0.162, and 0.208  $e^2b^2$  for  $^{132}\text{Xe}$ ,  $^{130}\text{Xe}$ ,  $^{128}\text{Xe}$ ,  $^{134}\text{Ba}$ ,  $^{132}\text{Ba}$ ,  $^{130}\text{Ba}$ ,  $^{136}\text{Ce}$ , and  $^{134}\text{Ce}$ , respectively, which are extracted from experimental values

in ref. [19]. The sign of  $e_c$  is determined to reproduce the ratios  $B(M1; I \rightarrow I - 1)/B(E2; I \rightarrow I - 2)$  for doubly odd nuclei, and is taken negative for all the nuclei. The reduced matrix element of the quadrupole operator for a neutron single hole or proton single particle is taken as

$$\langle j \| Q \| j \rangle = -\frac{\langle j \| r^2 Y^{(2)} \| j \rangle}{\sqrt{5}}, \quad (13)$$

where the harmonic oscillator basis states with the oscillator parameter  $b = 1.005A^{1/6}$  fm is used for the calculation of  $r^2$ . The effective charges are  $e_\nu = -1.0e$  and  $e_\pi = +2.0e$ , which are the values adopted in the previous studies [13–15].

The  $g$ -factor of the collective core in eq. (9) is determined using the magnetic dipole moment  $\mu$  of the  $2_1^+$  state in the neighboring even-even nuclei ( $N + 1, Z - 1$ ) as

$$g_c = \frac{1}{4} \sqrt{\frac{\pi}{3}} \mu(2_1^+), \quad (14)$$

where the adopted dipole moment,  $\mu(2_1^+)$ , is  $+0.76 \mu_N$  for all the nuclei, which is the mean value of the experimental data of  $^{132}\text{Xe}$ ,  $^{130}\text{Xe}$ ,  $^{128}\text{Xe}$ ,  $^{134}\text{Ba}$ ,  $^{132}\text{Ba}$  and  $^{130}\text{Ba}$ . The adopted  $g$ -factors for neutrons and protons are  $g_{\ell\nu} = 0.00$ ,  $g_{\ell\pi} = 1.00$ ,  $g_{s\nu} = -2.68$  and  $g_{s\pi} = 3.91$ , which are the same as in the PTSM calculations [13–15].

In fig. 4, the theoretical transition ratios  $B(M1; I \rightarrow I - 1)/B(E2; I \rightarrow I - 2)$  for the yrast states are compared with experiment. For  $^{132}\text{Cs}$ , the absolute  $B(M1)/B(E2)$  ratios of the  $13_1^+$ ,  $15_1^+$  and  $17_1^+$  states are larger compared to experimental data, but the staggering pattern is in phase with experiment. Concerning  $^{130}\text{Cs}$ ,  $^{128}\text{Cs}$ ,  $^{134}\text{La}$ , and  $^{136}\text{Pr}$ , large-amplitude staggering of the  $B(M1)/B(E2)$  ratios are in good agreement with the experimental data. In contrast with the cases for the nuclei discussed above, the experimental  $B(M1)/B(E2)$  ratios vary smoothly as a function of spin  $I$  for  $^{132}\text{La}$ ,  $^{130}\text{La}$  and  $^{134}\text{Pr}$ . The theoretical  $B(M1)/B(E2)$  ratios agree with the experimentally observed values.

In the PTSM the  $B(E2)$  values of yrare bands are roughly one half those of yrast bands [14]. However, this generic feature is not retained in the QCM because in the present version only one even-even core is assumed. In the forthcoming paper we will explicitly list all the  $E2$  and  $M1$  transition strengths.

To deepen our understanding of the excitation mechanism of the yrast and yrare states, we calculate effective angles between two angular momenta of a neutron and a proton. The effective angle  $\theta$  is defined as

$$\cos \theta = \frac{\langle \Phi(I\eta) | j_\nu \cdot j_\pi | \Phi(I\eta) \rangle}{\sqrt{\langle \Phi(I\eta) | j_\nu^2 | \Phi(I\eta) \rangle \langle \Phi(I\eta) | j_\pi^2 | \Phi(I\eta) \rangle}}, \quad (15)$$

where  $j_\nu$  and  $j_\pi$  are the angular-momentum operators for the neutron and the proton, respectively. The effective angle  $\theta$  turns out to be  $32^\circ$ ,  $57^\circ$ ,  $75^\circ$  and  $90^\circ$  for the particle-hole state with angular momenta  $L = 11, 10, 9$  and  $8$ , respectively, as given in the appendix of ref. [14].

In fig. 5, the calculated effective angles  $\theta$  for the yrast and yrare states of  $^{134}\text{La}$  ( $\kappa_{c\nu} = -0.8$ ,  $\kappa_{c\pi} = -0.4$ , and  $\kappa_{\nu\pi} = 6.0$ ) and  $^{134}\text{Pr}$  ( $\kappa_{c\nu} = -1.9$ ,  $\kappa_{c\pi} = -0.1$ , and  $\kappa_{\nu\pi} =$

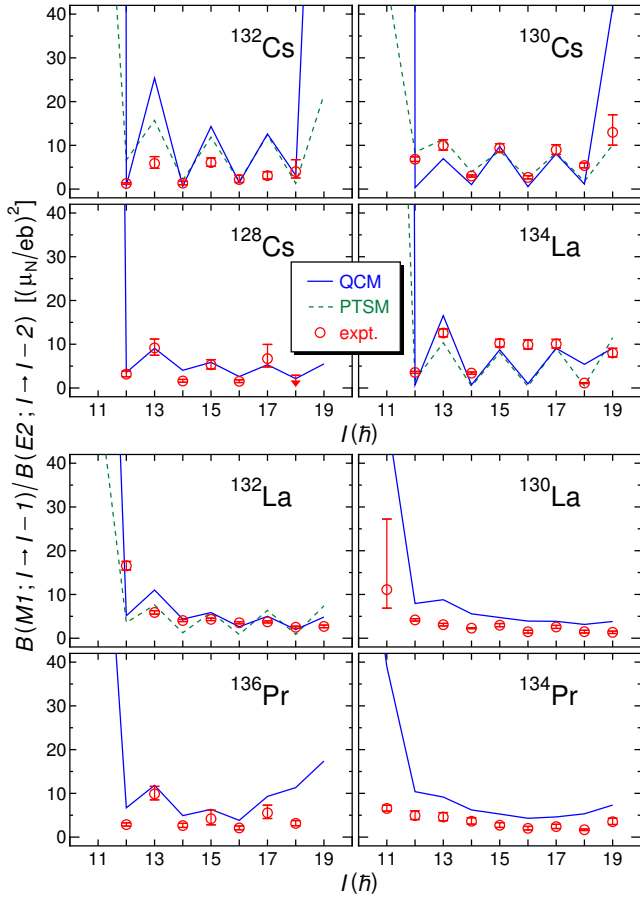


**Fig. 4.** Comparison of the calculated  $B(M1)/B(E2)$  ratios for the yrast states with experiment. Solid lines represent the results of the QCM, and dashed lines, those of the PTSM given in refs. [13–15]. Experimental data are taken from refs. [2, 3, 5, 6, 16–18, 20].

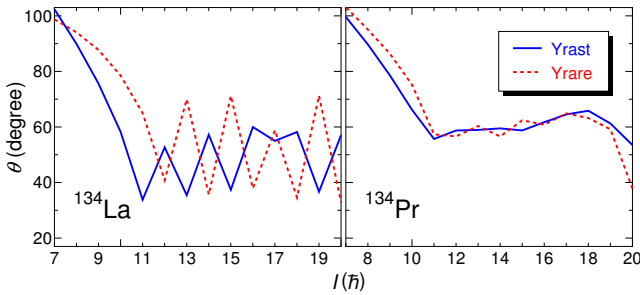


**Fig. 5.** The effective angles of two angular momenta as functions of the spin  $I$ , calculated in the QCM. Solid lines indicate the effective angles for the yrast states, and dotted lines, those for the yrare states.

7.0) are shown as functions of spin  $I$ . It is seen from the figure that the different features of  $^{134}\text{La}$  and  $^{134}\text{Pr}$  are significant. In the case of  $^{134}\text{La}$ , the angle  $\theta$  staggers as a function of spin  $I$ , which indicates that the angular momenta of the neutron and the proton open and close like a pair of chopsticks as a function of spin  $I$ . In the case of  $^{134}\text{Pr}$  the angle  $\theta$  decreases monotonically until the angular momen-

tum 11 and becomes almost a plateau to get no staggering. Thus, it is confirmed from our theoretical investigation that the staggering of the  $B(M1)/B(E2)$  ratios is caused by the chopsticks motion of the two angular momenta of the neutron and the proton along the yrast line.

In the QCM the calculated effective angle between the core and the neutron, and that between the core and the proton decreases as the total spin increases for the yrast states. Eventually at high spin the three angular momenta point toward the same direction. Thus, we do not support any picture of chiral doublet bands.

In conclusion, we have proposed the quadrupole coupling model (QCM) with the core and a neutron and a proton for a description of doublet bands in doubly odd nuclei. The model has only a limited number of parameters which are linearly changed as functions of neutron and proton numbers. It has been shown that in spite of its simplicity the model describes well the staggering of the  $B(M1)/B(E2)$  ratios of the yrast bands, not to mention the energy spectra for various isotopes. By analyzing total wave functions it turns out that the staggering of the  $B(M1)/B(E2)$  ratios occurs only when the coupling of the core and the particles are weak and that the staggering is caused by a chopsticks motion of the neutron and proton angular momenta.

The authors would like to thank Dr M. Sugawara, Dr H. Nakada, and Dr T. Mizusaki for valuable discussions. One of the authors (KH) would like to thank JSPS Research Fellowships for Young Scientists.

## References

1. K. Starosta *et al.*, Phys. Rev. Lett. **86**, 971 (2001).
2. R.A. Bark *et al.*, Nucl. Phys. A **691**, 577 (2001).
3. K. Starosta *et al.*, Phys. Rev. C **65**, 044328 (2002).
4. T. Koike, K. Starosta, C.J. Chiara, D.B. Fossan, D.R. LaFosse, Phys. Rev. C **67**, 044319 (2003).
5. G. Rainovski *et al.*, Phys. Rev. C **68**, 024318 (2003).
6. A.J. Simons *et al.*, J. Phys. G **31**, 541 (2005).
7. S. Frauendorf, J. Meng, Nucl. Phys. A **617**, 131 (1997).
8. S. Brant, D. Vretenar, A. Ventura, Phys. Rev. C **69**, 017304 (2004).
9. E. Grodner *et al.*, Int. J. Mod. Phys. E **13**, 243 (2004).
10. J. Srebrny *et al.*, Acta Phys. Pol. B **36**, 1063 (2005).
11. D. Tonev *et al.*, Phys. Rev. Lett. **96**, 052501 (2006).
12. C.M. Petrache, G.B. Hagemann, I. Hamamoto, K. Starosta, Phys. Rev. Lett. **96**, 112502 (2006).
13. K. Higashiyama, N. Yoshinaga, Prog. Theor. Phys. **113**, 1139 (2005).
14. K. Higashiyama, N. Yoshinaga, K. Tanabe, Phys. Rev. C **72**, 024315 (2005).
15. N. Yoshinaga, K. Higashiyama, J. Phys. G **31**, S1455 (2005).
16. B. Singh, Nucl. Data Sheets **93**, 33 (2001).
17. C.M. Petrache *et al.*, Nucl. Phys. A **597**, 106 (1996).
18. C.M. Petrache *et al.*, Nucl. Phys. A **603**, 50 (1996).
19. S. Raman, C.W. Nestor jr., P. Tikkanen, At. Data Nucl. Data Tables **78**, 1 (2001).
20. E.S. Paul, D.B. Fossan, Y. Liang, R. Ma, N. Xu, Phys. Rev. C **40**, 619 (1989).